Submonolayer alloying of copper on vicinal platinum: A combined atom and ion scattering study

D. A. MacLaren,* R. T. Bacon, and W. Allison
Cavendish Laboratory, University of Cambridge, Madingley Road, Cambridge CB3 0HE, United Kingdom

D. J. O'Connor and P. C. Dastoor
School of Mathematical and Physical Sciences, University of Newcastle, Callaghan, New South Wales 2308, Australia

T. C. Q. Noakes and P. Bailey
CCLRC Daresbury Laboratory, Daresbury, Warrington, WA4 4AD, United Kingdom

(Received 29 March 2004; revised manuscript received 11 June 2004; published 7 September 2004)

We present a combined helium atom scattering (HAS) and medium energy ion scattering (MEIS) study to provide a detailed description of sub-monolayer growth of copper on vicinal platinum. Initial growth is epitaxial but induces a small relaxation in the substrate. A strong temperature dependence of growth is observed and MEIS indicates the formation of a thin (two-layer) alloy between 450 K and 500 K. *In-situ* HAS measurements allow for the direct observation of alloying and reveal that it occurs in two unusually sharp phase transitions. Both HAS and MEIS indicate the onset of bulk alloying and dissolution of copper at surface temperatures above 600 K.

DOI: 10.1103/PhysRevB.70.125403 PACS number(s): 68.49.Bc, 68.49.Sf, 68.55.−a, 81.15.Hi

I. INTRODUCTION

Vicinal surfaces have a staircase-structure of crystalline terraces separated by atomic-scale steps that can, even at low densities, dominate surface functionality. Both the periodic structure and the unique, spatially-defined reactivity can be exploited and have been recognized to hold tremendous technological potential. For example, vicinal surfaces can be used as precusors for novel alloy, thin-film or molecular adsorbate structures and are candidate templates for nanoscale device fabrication.[1–3] In this report, we discuss the initial growth and alloying of thin copper films on vicinal platinum(111), considering exclusively the submonolayer regime. The copper-platinum(111) system is interesting because it has previously been observed to form ordered superstructures[4] whose properties could be tailored by the introduction of vicinality. A secondary aim of this study is to combine the perspectives of two independent but complementary surface-analytical techniques: medium energy ion scattering (MEIS) and helium atom scattering (HAS). MEIS has long been used to provide intricate layer-by-layer structural information and so is ideal for an analysis of surface alloying.[5] HAS, on the other hand, excels at probing lateral superstructures and is uniquely sensitive to variations in surface morphology.[6] We will demonstrate that these combined analyses enhance not only our understanding of surface phenomenology but also of the subtle contrast effects observed in both MEIS and HAS.

We will reference our results to the growth of copper on nominally flat Pt(111),[4,7] hereafter referred to as Cu/Pt(111), and Cu/Pt(997), a vicinal system which has been studied previously.[8] In the present work we use a vicinal surface aligned closer to the (111) plane than Pt(997) and with more than double the mean terrace width. The surface normal is inclined by 2.4° away from the (111) plane and towards the $[11\bar{2}]$ direction (Fig. 1). The surface consists of a regular array of (111) terraces, with a mean width of 54.4 Å and separated by monatomic, $[1\bar{1}1]$ microfacets. For convenience, we will refer to the surface as Pt(12 12 11).

For Cu/Pt(111), submonolayer growth characteristics are governed principally by the competing influences of the formation of strong Pt-Cu bonds and by the 8% lattice mismatch in the bulk structure. A commensurate, strained, two-dimensional overlayer is produced.[9] Although epitaxial growth is confirmed between 300 K and 450 K by the existence of sharp 1×1 LEED patterns,[9] HAS, scanning tunnelling microscopy (STM) and workfunction studies[4,7,10] indicate kinetic differences between growth at 340 K and at 450 K. At 340 K, both the HAS reflectivity[7] and the surface workfunction[10] decay monotonically during deposition, suggesting the formation of a rough copper adlayer. STM images[7] indicate two-dimensional, dendritic island growth, implying that Cu adatom diffusion across terraces and copper steps is facile, but that diffusion along kinked island and step edges is kinetically limited. As the copper coverage increases, these dendritic islands merge to form a defective two-dimensional layer, with a high vacancy density suppressing the HAS or workfunction oscillations generally ex-

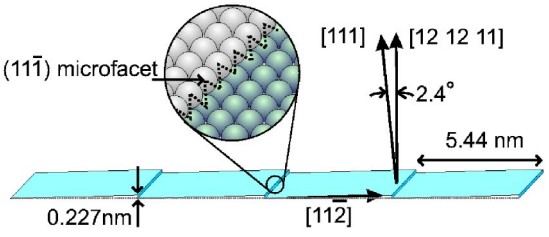

FIG. 1. Schematic of a Pt(12 12 11) step structure showing principal crystallographic directions.

pected for two-dimensional growth.[7] A HAS oscillation is observed, however, during growth at 450 K, where smooth, compact Cu islands can also be seen by STM,[4] thus indicating that the kinetic barrier to adatom migration about kinked Cu-Pt steps is overcome between 340 K and 450 K.

The introduction of surface steps can alter both the growth and the alloying characteristics of a thin film. For example, a recent HAS study of the Cu/Pt(997) system suggested that copper growth proceeds by step decoration and the formation of ordered, one-dimensional atomic chains aligned along the substrate step edges.[8] In contrast to Cu/Pt(111), a strong oscillation in HAS reflectivity confirmed the production of smooth sub-monolayer films at 350 K, demonstrating that surface vicinality has altered growth kinetics to improve thin film morphology.

The present study extends previous work in two key respects. First, we will use elemental-specific MEIS data to discuss the details of surface alloy formation. We will demonstrate a rich variation in alloy characteristics that are critical in determining the growth mode but have not been discussed previously. Second, the vicinal crystal used here has a different step density to either Pt(111) or Pt(997) and so is expected to interact with strain-relief mechanisms in the growing copper film in a distinct manner. As we will show, the intermediate step density studied gives rise to intermediate kinetics.

II. EXPERIMENTAL

MEIS measurements were taken at the UK National MEIS facility, CCLRC Daresbury Laboratory, while HAS was performed at the University of Cambridge. Both facilities have been described in detail previously.[11,12] At Daresbury, the sample was studied using a collimated 100 keV hydrogen ion beam, with the backscattered ion signal detected by a toroidal electrostatic analyzer. Three double-aligned, low-index scattering geometries were chosen to afford layer-specific structural analysis[13] and are sketched in Fig. 2. The geometries allow the uppermost layer [[110] incidence, Fig. 2(a)], first two layers [[211] incidence, Fig. 2(b)] or the first 3 layers [[411] incidence, Fig. 2(c)] to be probed selectively. Typically, the sample received an ion dose of 10^{16} ions cm^{-2} per data set, after which the the sample was moved to a new position. As the copper overlayer has a smaller mass than platinum, all MEIS spectra have the Cu elastic signal superimposed onto a strong "background" deriving from inelastic scattering from Pt. In elemental analysis, great care was taken to separate Cu and Pt components and a detailed description of the data analysis can be found elsewhere.[14]

HAS measurements were performed using a temperature-controlled supersonic expansion atom-beam source with an energy between 14 meV and 80 meV ($\lambda = 0.5$ to 1.3 Å). Scattering was generally about a "Bragg antiphase position," where helium atoms scattering from successive terraces of the vicinal crystal interfere destructively.[6] These conditions were chosen to maximize the intensity contrast during growth and are sensitive to changes in both defect density and step height distribution.[6] For the incident wavevectors

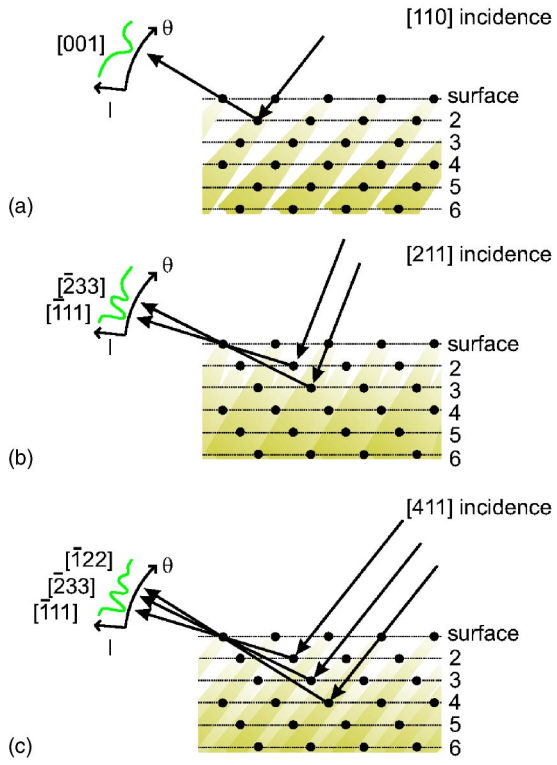

FIG. 2. MEIS double-aligned scattering geometries. (a) One-layer illumination: [110] incidence; $[\bar{1}\bar{1}2]$ surface direction; 73–93° detected scattering angle. (b) Two-layer illumination: [211] incidence; $[\bar{2}11]$ surface direction; 87–107° detected scattering angle. (c) Three-layer illumination: [411] incidence; $[\bar{2}11]$ surface direction; 71–91° detected scattering angle.

here, the stepped crystal produced two or three diffracted beams that were tilted slightly from the macroscopic specular direction and overlapped to form a broadened "specular" beam aligned along the in-plane scattering axis. In a later section, we will discuss the lateral surface order by presenting spot-profiles of the diffracted helium beam. Such scans were obtained by rastering the detector across the specular helium peak for the in-plane axis while rocking the crystal out of plane to build a two-dimensional image.

The same vicinal platinum single crystal (Surface Preparation Laboratory, The Netherlands) was used for both sets of experiments. It was prepared *in-situ* by repeated argon ion bombardment (800 eV, 30 min), and annealing (800 K, 30 min), with an initial oxygen treatment (30 min, 10^{-6} mbar oxygen, 800 K, followed by a flash anneal at 1000 K) to remove residual carbon. Crystal quality was checked by LEED and Auger electron spectroscopy (Daresbury) or by the observation of a reproducibly intense, sharp helium reflectivity (Cambridge). Diffraction scans of the clean surface prior to copper deposition indicated a well-ordered step distribution with a fitted mean step separation of 50.0 nm. Over a period of several months, the mean step separation was observed to increase, suggesting the onset of step bunching. This gradual phenomenon did not result in a gradual variation in growth characteristics and does not impact on the results presented here. A more detailed HAS and STM study

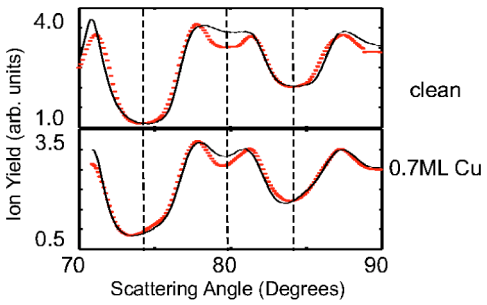

FIG. 3. [411] geometry MEIS spectra of clean Pt(12 12 11) and ~0.7 ML Cu/Pt(12 12 11) grown at 300 K. Each panel displays both the detected ion current (dots) and the best-fit VEGAS simulation (full line). Simulations to Cu growth are calculated as a linear combination of clean and Cu-covered substrate, assuming a commensurate structure. Dashed vertical lines are to guide the eye and indicate the approximate center of blocking dips for clean Pt(12 12 11). In each case, Cu/Pt(12 12 11) and clean Pt(12 12 11) dips do not align.

of this process is currently in progress and the results will be presented elsewhere.[15] Copper deposition was performed using water-cooled electron-bombardment evaporators while maintaining the chamber pressure below 10^{-9} mbar. At Daresbury, the evaporated flux was monitored by measuring the ion current leaving the evaporator cell, using the MEIS data itself for calibration. The approximate flux was ~0.35 ML min^{-1}. In Cambridge, calibration was performed by direct observation of monolayer- completion oscillations of the specular helium reflectivity, which indicated a mean deposition flux of ~0.60 ML min^{-1}.

III. RESULTS AND DISCUSSION

A. MEIS of 0.5 ML Cu/Pt(12 12 11)

In a previous study, we determined that the clean Pt(12 12 11) surface has no lateral reconstruction and only a very small inter-layer reconstruction.[14] Unusually, the first interlayer spacing is increased by 0.04 Å with respect to the bulk while the second interlayer spacing is decreased by 0.02 Å. The results suggest that strain effects in the Pt(12 12 11) surface are close to those observed on Pt(111), where a similar vertical reconstruction was observed by LEED.[16] We observed no additional relaxations introduced by the surface vicinality.

Figure 3 plots the [411] MEIS spectra for Pt(12 12 11) before and after room-temperature (300 K) deposition of ~0.7 ML copper. Similar plots were obtained for the other two geometries.[14] Both data sets give the angular variation of ions scattered elastically from Pt. They exhibit strong blocking-dips, as expected for the double-aligned geometries chosen.[5] The Cu/Pt(12 12 11) trace does not have *additional* blocking features with respect to the clean Pt spectrum, so crystallographic ordering is maintained. However, with respect to the clean surface, the blocking dips exhibit a slight shift towards smaller angles, indicative of a surface relaxation. No blocking features were observed in the background-subtracted elastic peak from Cu, implying that all of the copper resides on the first layer and that there are no three-dimensional copper structures. The data is therefore consistent with a relaxed, commensurate and two-dimensional overlayer, similar to the growth of Co/Pt(111)[17] and Ni/Pt(111),[18] which have comparable lattice mismatches.

Also plotted in Fig. 3 is a best-fit simulation to all MEIS data, generated by the VEGAS simulation program[19] and discussed in more detail in the following section. An excellent fit is obtained by assuming commensurate, island growth and without the need for lateral surface reconstruction or intermixing. The simulation yields a surface relaxation of (-0.16 ± 0.02) Å for the copper-covered platinum, reversing the extension observed on the clean Pt(12 12 11) surface. A contraction of (-0.02 ± 0.02) Å is observed in the second interlayer spacing, unchanged from the clean surface. The observed interlayer contraction is much larger than that seen for Co/Pt(111),[17] but in accordance with the 8% in-plane lattice relaxation induced by commensurate growth.

B. MEIS of submonolayer annealing

While VEGAS gives good fits to the MEIS spectra for submonolayer copper films grown at 300 K, thin films grown at 400 K are not well-described by assuming two-dimensional copper overlayers. Epitaxial growth models result in poor fits to the experimental data. Thus, it is likely that copper growth at 400 K results in a significant degree of intermixing of Cu and Pt and the formation of a thin alloy layer. To understand the process better, the following experiment was conducted. A ~0.8 ML Cu film was grown at a sample temperature of 150 K and the MEIS spectra recorded. The sample was then heated rapidly to a chosen "anneal temperature," held for 5 minutes, then cooled rapidly back to 150 K once more. A single MEIS spectrum was recorded in the [411] geometry for each anneal temperature and the whole process was repeated to selected temperatures up to 650 K.

A compositional analysis of the uppermost three atomic layers was performed by best-fitting energy-projections of the MEIS spectra about the layer-specific blocking dips. Details of the analysis are as follows. In the [411] geometry, layer by layer information was obtained by determining the Cu/Pt yield for three exit geometries which reveal selectively the first (74.21° scattering), the first two (84.24° scattering) and the first three (90° scattering) atomic layers—see Figs. 2 and 3. For these geometries we should, in principle, see one, two and three atoms per row, respectively, and the ratio of Cu/Pt for each would allow the layer-by-layer concentration to be determined.[5] In reality, atomic thermal vibrations allow deeper layers to be illuminated and therefore contribute to the scattering yield. Using VEGAS and thermal vibration amplitudes fitted to the clean Pt(12 12 11) data,[14] realistic yields were obtained for Cu and Pt from a number of modelled surface compositions. It was assumed that during annealing the copper would be on the surface, or diffused into the second or deeper layers. As the coverage was less than one monolayer, measured MEIS spectra derive from both copper-covered and "clean" patches of the surface. Be-

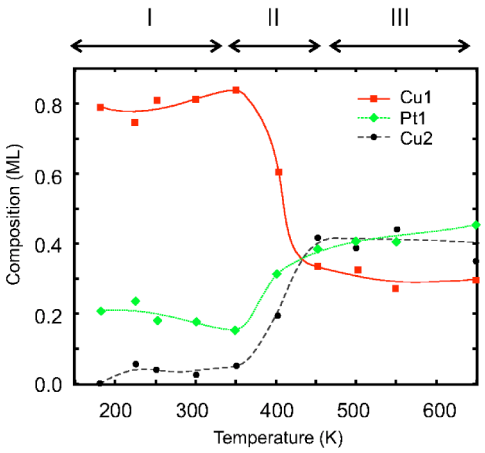

FIG. 4. MEIS "annealing curves" for nominal 0.8 ML Cu/Pt(12 12 11) grown at 180 K. Layer-specific elemental concentrations are plotted as a function of anneal temperature, as calculated from MEIS yields from scattering in the three-layer geometry. Cu1 and Cu2 are the coverages of copper in the first and second atomic layers, respectively. Pt1 is the coverage of platinum in the first layer. Three temperature regimes, as discussed in the text, are indicated at the top of the figure.

fore the onset of alloying, this superposition of spectra was observed to give asymmetric, distorted blocking features, particularly for the $[\bar{1}11]$ feature (in the angular range of $73°-75°$) for the [411] geometry (Fig. 3). Simulations were therefore obtained for clean Pt(12 12 11), a monolayer of copper as the surface atomic layer of Pt(12 12 11) and a monolayer of copper as the second atomic layer of Pt(12 12 11), with the surface layer being pure platinum. In this fitting process, the concentration of copper was a free parameter so no prior assumption was made about the coverage.

Summarized results of the MEIS analysis are presented in Fig. 4, which plots the calculated copper concentrations in the first atomic layer ("Cu1") and second atomic layer ("Cu2") as a function of anneal temperature. Also plotted is the surface concentration of platinum ("Pt1"). Three distinct temperature regimes are distinguishable.

Between 180 K and 350 K ("regime I"), the layer-specific elemental composition is static. Figure 4 indicates that the majority of copper, with a fitted coverage of (0.80 ± 0.05) ML, resides on the surface and there is no evidence of intermixing. The coverage of copper in the second layer, Cu2, is effectively zero. As discussed in the previous section, the fitted elastic yield for the Cu component (not shown) exhibits no strong blocking features in this temperature range, indicative of a lack of either three-dimensional copper structures or copper on the second atomic layer.

The second key temperature regime ("regime II") is between 350 K and 450 K, where Fig. 4 indicates a clear transition. In this temperature regime there is significant movement of Cu from the first to the second layers and the Cu yield for the first atomic layer drops by 50%. Blocking features in the background-subtracted elastic Cu yield (not shown) are observed very weakly at 400 K and more substantially at 450 K, consistent with the Cu moving subsurface, however, no *additional* blocking features are observed, so crystallographic ordering is maintained. In the annealing process all minima shift to a lower angle, which suggests a contraction of the surface layer. Surface composition must also become more homogeneous: we observe the minima to become more symmetric and lose their distorted appearance (Fig. 3), which arose from the superposition of signals from distinct clean and copper-covered patches of the surface. The MEIS data therefore indicate the formation of a relaxed substitutional alloy phase with the lateral spacing of the Pt lattice.

The third key temperature regime is above 450 K ("regime III"). Between 450 K and 650 K, little variation is observed in the MEIS spectra, suggesting that the alloy phase formed in regime II is relatively stable. An analysis was not performed above 650 K, where the Cu signal weakened—a feature suggesting the onset of dissolution of Cu into the bulk crystal. In summary, the MEIS annealing curves are consistent with the formation, then dissolution, of a thin film alloy. Between annealing temperatures of 180 K and 350 K, any alteration to the thin film structure is restricted to the uppermost atomic layer alone. Around an anneal temperature of 350–450 K, a distinct phase change is observed, which compositional analysis suggests is either the formation of a thin, two-layer alloy or of a reconstruction of the outermost layers. Thin alloy formation has also been observed in submonolayer Co/Pt(111),[8] Ni/Pt(111)[20] and Ag/Pt(111),[21] which may be expected to behave similarly to the chemically-similar Cu/Pt(111) system. Above 650 K, the Cu elastic signal (not shown) weakens, indicating the onset of dissolution of Cu into the bulk.

C. HAS of Cu/Pt(12 12 11) growth

Figure 5 plots the helium reflectivity of Pt(12 12 11) during the first three monolayers of copper film growth at a range of surface temperatures. Data sets were repeated several times to establish the reproducibility of the evaporator and facilitate the calibration of copper deposition rates, using the strong maxima in the 300 K and 420 K(Ref. 4) trends to define monolayer coverage. The data indicate clear monolayer-completion features at all growth temperatures between 200 K and 520 K and there is a significant temperature dependence for sub-monolayer growth. Although not the focus of this study, the data also indicate that growth of Cu/Pt(12 12 11) above one monolayer involves significant changes in surface morphology. This observation is in contrast to that of Cu/Pt(997) and will be discussed in more detail elsewhere.[15]

Differences between succcessive curves of Fig. 5 can be attributed to succesive kinetic barriers to adatom motion being overcome as temperature increases. Following the approach of the previous section, we will describe the data by dividing submonolayer growth into the same three temperature regimes: I ($T<350$ K); II ($350\ \text{K}<T<450$ K); and III ($T>450$ K).

At a sample temperature of 200 K (regime I), copper deposition causes a slow decay in specular reflectivity, with a shoulder at 1 ML, then monotonic decay with increasing film thickness, achieving a terminal reflectivity around 5% of that

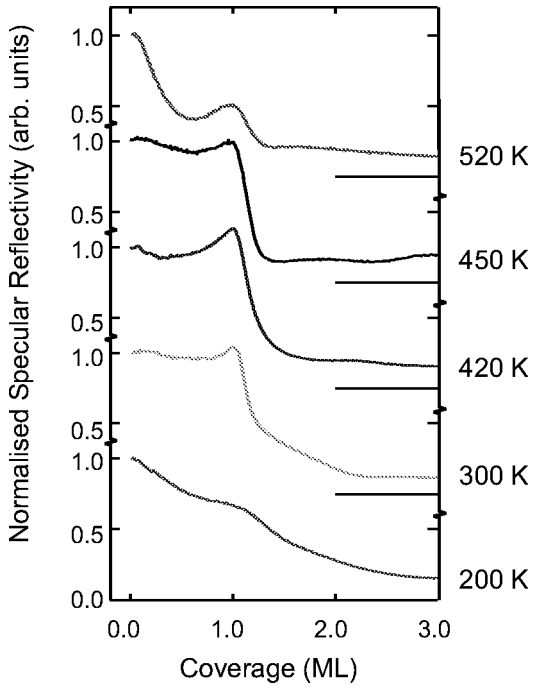

FIG. 5. Normalized helium reflectivity of Pt(12 12 11) during the thin-film deposition of copper. Taken under Bragg antiphase conditions for clean Pt(12 12 11) ($\lambda = 0.59$ Å, 62.8° incidence), scattering along the $[11\bar{2}]$ direction and with uniform deposition flux. Maxima in the 300 K and 420 K trends were used to calibrate the flux required for monolayer coverage for all data sets.

of the clean surface. Substantial surface roughening occurs during growth, but the weak monolayer-completion oscillation suggests a defective two-dimensional growth regime, at least for the first monolayer. Such a process is consistent with the lack of three-dimensional structures seen by MEIS at this temperature. Using the gradient of the decay and normalizing with respect to the substrate atomic density, we obtain a cross-section per deposited adatom of approximately 3.2 Å^2 for the first half monolayer and 1.3 Å^2 for the second half monolayer. Given that both of these values are an order of magnitude smaller than the cross-section expected for isolated adatoms,[6] significant coalescence of the adsorbed copper into islands must have occurred. Nevertheless, the growth of these adatom islands continues to roughen the surface with time, indicating a continued increase in surface step density. The data is, therefore, consistent with the formation of dendritic step-decorations, similar to those observed by STM for the Cu/Pt(111) system at 340 K.[7] It is interesting to note, however, that the attenuation of reflectivity is slower than that of the Cu/Pt(111) system at 340 K and gives a more pronounced monolayer-completion feature. Thus, Cu/Pt(12 12 11) films grown at 200 K appear less defective than Cu/Pt(111) films grown at the higher temperature of 340 K.

Between 300 K (regime I) and 450 K (regime II), Fig. 5 shows a clear oscillation, with surface reflectivity at monolayer coverage equal to or better than that of the clean surface. During submonolayer growth, the relative magnitude of this oscillation does not exceed 10% (although a slightly more pronounced oscillation was observed on occasion, presumably due to variations in the substrate step distribution). Thus, the surface defect or step density does not change appreciably during submonolayer growth. The data, therefore, indicate a near-ideal step-flow mechanism, and smooth, defect-free step decoration. A comparison of the submonolayer behavior for 200 K (defective, rough 2D growth) and 300 K (smooth, step-flow growth) therefore suggests that the kinetic barrier for adatom motion about Cu step edges on Pt is overcome within temperature regime I. Although no clear variation was observed throughout regime I by MEIS (Fig. 4) the HAS data here indicates a smooth transition of the growth mode. In contrast, the HAS data of Fig. 5 does not alter substantially throughout temperature regime II, which the MEIS data of Fig. 4 has indicated to straddle an alloying transition. Thus, the combination of the two data sets reveals far more information than either set alone.

Finally, for growth at 520 K (regime III), a 60% signal attenuation at a coverage of 0.5 ML indicates that surface roughening commences immediately upon deposition. A small maximum at 1 ML is followed by a decay to damped growth oscillations. The initial attenuation rate suggests a "cross-section per adatom" of approximately 11.0 Å^2, which is far larger than that measured at lower temperatures and indicates a variation in the growth mode. Near-perfect step-flow growth was observed at lower temperatures, so no kinetic barriers—such as barriers to surface diffusion or step-crossing—remain for Cu adatom motion *along* the surface. The mechanism for surface roughening is more likely, therefore, to arise from the onset of alloying or surface reconstruction. Between 450 K and 520 K, the kinetic barrier to Cu adatom motion *into* the substrate, either by incorporation into or exchange with the uppermost Pt layer, must be overcome. Intermixing must then cause a buckling of the surface to account for the increased diffuse scattering observed. A similar effect is observed to occur in the Ag/Pt(111) system at 620 K,[22] where localized corrugations are generated about adislands and where alloying initiates at step edges.[23]

A comparison between Fig. 4 and HAS data of the literature for flat Pt(111) (at 340 K and 420 K)[4,7] and vicinal Pt(111) (at 350 K only)[8] allows for the impact of vicinality on copper thin film growth to be assessed. For "room temperature" submonolayer growth on Pt(111), an immediate, monotonic and rapid decay in helium specular reflectivity is observed;[7] the present work indicates a weak monolayer-completion oscillation; and for Pt(997), there is a strong monolayer-completion oscillation.[8] Thus, for the Cu/Pt(111) system, the degree of surface vicinality does have a strong influence on the growth mode and, unlike the Co/Pt(111)[24] system, lowers the temperature required for smooth submonolayer growth.

It is interesting to consider the mechanism for improved thin film growth. On vicinal Pt(997), impinging adatoms are thought to migrate rapidly to vicinal step edges, growing in an initially row-by-row manner to form "atomic wires."[8] A monolayer-completion oscillation indicates that growth roughens towards half-monolayer coverage, regaining a low defect concentration at monolayer completion. For Cu/Pt(111), on the other hand, the surface roughens throughout film growth at room temperature. STM images of

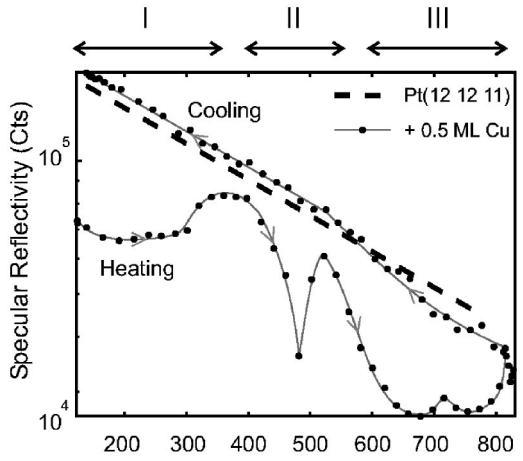

FIG. 6. HAS "annealing curve" of 0.5 ML Cu/Pt(12 12 11) grown at 180 K and heated at $\sim$10 K min^{-1} to 800 K, then cooled. Taken under Bragg antiphase conditions for clean Pt(12 12 11): $\lambda = 1.07$ Å, 53.8° incidence, $[11\bar{2}]$ direction. The grey line is to guide the eye only. The thicker dashed line is an exponential fit to data taken from clean Pt(12 12 11).

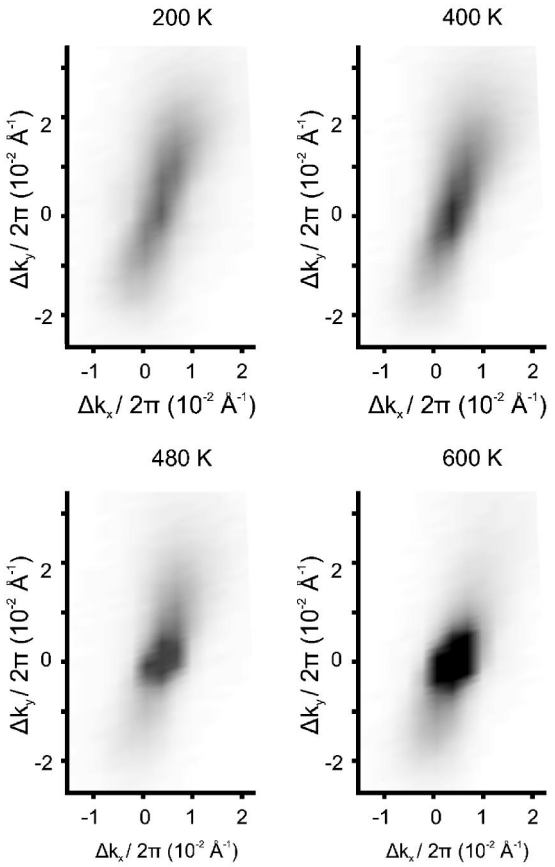

FIG. 7. Spot-profile of the specular helium reflection about a Bragg position ($\lambda = 1.07$ Å, 61.8° incidence) for selected anneal temperatures. Scan size is ±2° in-plane; ±1° out of plane. The $[11\bar{2}]$ surface direction lies along the long axis of each spot. Shading is linear greyscale from low (white) to high (black).

Cu/Pt(111) indicate that roughening arises from the growth of dendritic islands, which have a large diffuse-scattering cross section to HAS. Dendritic growth is attributed to a kinetic barrer for adatom motion about kinked step edges, so that arriving adatoms are unable to migrate about an island perimeter to an optimal position. Interestingly, a similar process might be expected to occur—*but evidently does not*—along Cu-decorated steps on vicinal Pt(111). There are two likely possibilities for the change in growth mode. First, Cu-decorated steps may have a very low kink density, such that compact island formation is not impeded. A static kink density would be consistent with the only slight variation in helium specular reflectivity observed during submonolayer growth. Alternatively, intermixing may occur at the step edges, with a low concentration of Pt migrating outwards with the growing Cu film and acting as a surfactant. In-plane intermixing could explain the similarity of the HAS traces for growth at 300 K and 420 K, temperatures which straddle the onset of alloying observed in Fig. 4. Such step-mediated intermixing has been observed in both the Ag/Pt(111)[23] and Ni/Pt(997)[20] systems, but at low concentrations would not be observable by MEIS.

D. HAS of submonolayer annealing

Our HAS study of annealed Cu/Pt(12 12 11) was conducted in a slightly different manner to the MEIS experiment outlined above. A 0.5 ML Cu film was deposited at a sample temperature of 180 K. The surface's specular reflectivity was then monitored at a Bragg antiphase angle as the sample was heated, then cooled, *continuously* from 120 K to 800 K to 120 K at a linear rate of $\sim \pm 10$ K min^{-1}. In comparison to the "heat, hold, cool" cycles of the MEIS experiment, we may therefore expect phase transitions to shift to slightly higher temperatures than observed in Fig. 4. Each datum was recorded following re-optimization of the crystal's angular alignment in both in- and out-of-plane scattering axes. This procedure allowed us to "track" the diffracted beams and ensured that the observed variations could be attributed to changes in surface morphology rather than to a gradual misalignment of the detector with respect to the specular intensity. Consequently, interference effects arising from a gradual variation in the step distribution cannot account for large contrast variations. Results are presented in Fig. 6, which also presents data for the clean surface. The reflectivity of clean Pt(12 12 11) (Fig. 6, dashed line) varies exponentially with temperature, in accordance with Debye-Waller attenuation,[6] so appears as a linear trend when plotted on the logarithmic scale. There are no significant deviations from the exponential trend in the temperature range studied and so no significant structural alteration occurs. In contrast, significant deviations from the exponential trend are observed for Cu/Pt(12 12 11) (Fig. 6, solid line and dots). As we will discuss below, all such deviations indicate an alteration to surface morphology, most likely due to a change in surface diffuse-scattering cross-section or in the surface Debye temperature.

Following the annealing experiment, the surface was cleaned and an identical film was prepared. A HAS spot-profile analysis was then performed following anneals at key

temperatures in the data. Results are presented in Fig. 7 and will be discussed alongside Fig. 6.

Figure 6 indicates several phase changes during the annealing 0.5 ML Cu/Pt(12 12 11). The phase changes are irreversible since heating (lower) and cooling (upper) curves do not coincide. As with the discussion of previous sections, we split the annealing behavior in Fig. 6 into three temperature regimes, as indicated at the top of the figure.

As before, regime I covers temperatures up to 350 K and we will show to be restricted to Cu adatom rearrangment. There is an immediate deviation from the linear decrease in surface reflectivity expected for simple Debye-Waller attenuation. The increase in specular reflectivity arises from a decrease in diffuse scattering of helium from the surface. It can therefore be interpreted as a decrease in surface defect density, either because defects are being removed from the surface or because defects are mobile and coalesce to reduce their net scattering cross-sections. The increase in specular reflectivity (relative to the Debye-Waller expectation) is significant by the time surface temperature reaches 300 K. Correcting for the thermal variation, we calculate that the 'scattering cross-section per adatom' halves between 200 K and 400 K. The variation seems consistent with the differences between the 200 K and 300 K growth curves of Fig. 4: at 200 K, deposition of 0.5 ML of adatoms decreases reflectivity substantially, whilst at 300 K, little variation of reflectivity is observed. In comparison to the timescales for elementary surface reactions, the intensity variations in this first regime are relatively slow. For example, the heating rate of 10 K min^{-1} is far slower than those generally used for thermal desorption spectroscopy (TDS) studies of elemental reactions, yet the feature is much broader than typical TDS peaks. Under these conditions, thermally activated, low-order processes occurring with a typical attempt frequency of 10^{13} Hz would give rise to a far sharper feature than the gradual change observed in regime I.[25] In contrast, the long, slow process observed here hints at either several concerted processes or a process that is limited by mass-transfer and signficant surface rearrangement.

The first two panels of Fig. 7 plot the helium spot-profile obtained from the 0.5 ML Cu/Pt(12 12 11) surface before and after annealing to 400 K. Both images were taken at the same temperature and at a Bragg angle for the vicinal Pt surface, in order to minimize streaking of the spot due to scattering across Pt-Pt steps. Scattering across hetero-steps (i.e., Cu-Pt steps), however, will not be exactly in-phase and the phase-shift in the scattered beam will cause streaking of the spot profile in the direction of those steps. Note that under the scattering conditions used, diffracted beams do not appear as discrete maxima, rather contribute to a single "specular" beam that is broadened along an axis perpendicular to the step edges. A comparison of first two panels of Fig. 7 shows that the intensity for the 400 K spot is higher than that of the 200 K spot, in agreement with the surface smoothing discussed above. Nevertheless, both images retain strong streaking along the $[11\bar{2}]$ direction ("downhill" on the vicinal surface), indicating the retention of Cu-Pt steps. The spot profile is relatively narrow perpendicular to the "downhill" direction, so adislands must align preferentially with the crystal miscut.

Combining the above MEIS and HAS results, we conclude that the intensity variations in regime I (Fig. 6) are attributable to adatom motion and reorganization of the outermost surface alone. Reflectivity changes are most likely due to the coalescence of two-dimensional Cu islands from rough, dendritic shapes to more compact, geometric forms. As both MEIS data and HAS uptake curves indicate two-dimensional growth, there will be few three-dimensional structures present on the surface; Cu adatoms crossing Cu steps is facile for both the rough, dendritic (and therefore kinked) steps at 200 K and the smoother step edges evident at 300 K. Evidently, Cu adatom motion across a Pt terrace must also be facile for 2D growth to occur. The main kinetic barrier that is overcome between 200 K and 300 K is most likely to be that of adatom motion along a kinked copper step/island edge, a necessary motion for island coalescence.

Returning to the HAS annealing curve, we identify the second temperature regime between 350 K and 520 K. As discussed previously, we attribute differences in the precise transition temperatures in Figs. 4 and 6 to the different annealing cycles used for the two experiments. Two strong, sharp and reproducible features centred around 480 K are evident in the HAS annealing curve. Correcting for thermal attenuation, the "scattering cross-section per adatom" approximately quadruples between 400 K and the reflectivity cusp. Such a dramatic variation in reflectivity across a relatively small temperature range is particularly interesting. Similar effects have not, to our knowledge, been reported using HAS data previously. For example, the analogous experiment conducted for the related system Ag/Pt(111) showed a single, monotonic variation and simple Debye-Waller exponential background.[21] Thus, there are clear, unambiguous differences between the growth of Cu/Pt(111) and of Ag/Pt(111), possibly driven by the change in the sign of the lattice mismatch for the two systems.

It is clear that regime II involves two discrete processes: one rapid process leading to substantial surface roughening; the second process leading to an equally rapid and dramatic smoothing of the surface. A comparison with the MEIS annealing data presented in Fig. 4 indicates that the two features centered on 480 K relate to the thin-film alloy formation that was observed to have occurred around 450 K with MEIS. Spot-profile analysis (Fig. 7, third panel) indicates a much more compact specular beam, with less streaking along the $[11\bar{2}]$ direction, suggesting the removal of Cu/Pt steps from the surface region and a return to Pt/Pt steps (or alloy steps with a similar height) dominating the perpendicular morphology. There are no satellite diffaction peaks and hence no evidence of an ordered superstructure, such as the dislocation network observed by Holst *et al.*[4] at higher coverages. Thus, any surface reconstruction must be localized and aperiodic. A consistent explanation for the sharp phase transition observed is that the formation of the thin alloy film observed by MEIS occurs by two processes. In terms of the comparison with thermal desorption spectroscopy discussed above, both processes occur on a far faster timescale than the adisland coalescence of regime I. The timescale is most consistent with a zeroth-order surface process, i.e., purely kinetically-limited and independent of surface coverage.

Such a mechanism is therefore unlikely to be mediated by surface steps, because it would then be limited by the timescale for adatom migration to the nearest step site. We believe it more likely to reflect direct alloying at terrace sites rather than step-mediated alloying. First, copper is incorporated into interstitial sites in the uppermost Pt layer, increasing lattice strain and causing localized, aperiodic corrugations that act to decrease specular reflectivity. A similar morphology is observed in thicker Cu/Pt(111) films, where the remaining Cu ad-islands adopt a dendritic profile, aligning along short dislocation lines in the underlying layer.[4] This strained surface must be highly unstable, because the surface roughening is removed as quickly as it was observed. The second rapid transition would then be the removal of copper adislands from the surface and the formation of the substitutional alloy observed by MEIS. Cu atoms adopt random lattice sites in the upper layer. This second process is consistent with the increase in specular reflectivity observed, the lack of strong streaking in the HAS spot profile and the lack of additional blocking features in the alloy's MEIS spectrum. Overall, then, the strong HAS contrast variations observed in regime II are consistent with a direct observation of the initial insertion of Cu adatoms into the platinum terrace.

The third temperature regime identified is from 520 K to 800 K. As annealing continues, a strong attenuation is observed in sample reflectivity, consistent with the decline in intensity observed during thin film growth at 520 K (Fig. 4). It is unclear whether the increased gradient is attributable to continual surface roughening or is simply characteristic of a decreased Debye temperature for the thin film alloy. We attribute two clear peaks, at 720 K and 800 K, to subsequent alloy phases and the onset of bulk alloying—the complete dissolution of copper into the substrate. Although, strictly, HAS is only sensitive to alteration in surface morphology, we assume that the annealing processes driving bulk alloying also act to anneal and smooth the surface layer. Certainly, the features observed correspond to the temperature range within which the copper MEIS signal weakened and ultimately was lost, which again indicates the process of bulk alloying.

Finally, upon cooling down (upper curve), the surface reflectivity is much higher than during the annealing process, illustrating the irreversible nature of the phase changes observed. A true exponential trend is not achieved until the surface temperature is lower than 500 K. This feature is presumably attributable to incomplete alloying and annealing processes which are not frozen-out until 500 K. Below 500 K, surface reflectivity follows a very similar trend to that of the clean Pt(12 12 11) surface. The slightly higher absolute intensity is likely due to differences in surface preparation from one day to the next, but the similarity in gradients indicates a similar Debye surface temperature and therefore the almost complete dissolution of surface copper.

IV. CONCLUSION

We have provided a detailed description of the early stages of growth and alloying of Cu/Pt(12 12 11) for the first time. Both medium energy ion scattering and helium atom scattering indicate that growth can be described in three distinct regimes. The growth of copper on platinum (12 12 11) proceeds by imperfect epitaxy at 200 K and ideal stepflow between 300 K and 450 K. Above 450 K, growth proceeds by direct alloy formation.

The Cu/Pt(12 12 11) system differs from both Cu/Pt(111) and Cu/Pt(997). The introduction of surface steps improves the quality of films with respect to Cu/Pt(111) in the submonolayer regime. Above one monolayer, on the other hand, the growth of Cu/Pt(12 12 11) appears more similar to Cu/Pt(111) than Cu/Pt(997), with the onset of substantial surface roughening. In general, many aspects of Cu growth are comparable to those of related Co, Ni, Ag or Pt on Pt(111) systems, with each system favoring low-temperature epitaxial growth but rich alloying behavior at higher temperatures. For Cu, we used helium atom scattering to provide a real-time observation of initial alloy formation, which we demonstrate to occur in a novel, 2-stage process around 450 K. It is clear that further, a spatially-resolved analysis of these phase transitions would be particularly interesting.

More generally, helium atom scattering and medium energy ion scattering have proved an ideal combination of techniques for the study of thin-film growth and alloying, providing information on both surface and subsurface structure. The combination of techniques has allowed for the assignment of otherwise unidentifiable features in both data sets. In particular, strong contrast variations evident in HAS data allow for a rapid identification of alloy phase transitions whose nature can then be studied in more detail by complementary techniques such as MEIS.

The Engineering and Physical Sciences Research Council is thanked for financial support through Grant No. GR/R90512.

*Electronic address: dam30@cam.ac.uk; URL: http://www-sp.phy.cam.ac.uk

[1] K. Kuhnke and K. Kern, J. Phys.: Condens. Matter **15**, S3311 (2003).
[2] N. Neel, T. Maroutian, L. Douillard, and H.-J. Ernst, J. Phys.: Condens. Matter **15**, S3227 (2003).
[3] S. Rousset, V. Repain, G. Baudot, Y. Garreau, and J. Lecoeur, J. Phys.: Condens. Matter **15**, S3363 (2003).
[4] B. Holst, M. Nohlen, K. Wandelt, and W. Allison, Phys. Rev. B **58**, R10195 (1998).
[5] J. F. van der Veen, Surf. Sci. Rep. **5**, 199 (1985).
[6] D. Farías and K.-H. Rieder, Rep. Prog. Phys. **61**, 1575 (1998).
[7] B. Holst, M. Nohlen, K. Wandelt, and W. Allison, Surf. Sci. **377–379**, 891 (1997).
[8] P. Gambardella, M. Blanc, H. Brune, K. Kuhnke, and K. Kern, Phys. Rev. B **61**, 2254 (2000).

[9] M. T. Paffett, C. T. Campbell, T. N. Taylor, and S. Srinivasan, Surf. Sci. **154**, 284 (1985).
[10] M. Nohlen, M. Schmidt, and K. Wandelt, Surf. Sci. **331–333**, 902 (1995).
[11] P. Bailey, T. C. Q. Noakes, and D. P. Woodruff, Surf. Sci. **426**, 358 (1999).
[12] A. P. Graham, E. M. McCash, and W. Allison, Phys. Rev. B **51**, 5306 (1995).
[13] C. J. Baddeley, L. Bloxham, S. Laroze, R. Raval, T. Noakes, and P. Bailey, J. Phys. Chem. B **105**, 2766 (2001).
[14] D. J. O'Connor, D. A. MacLaren, T. C. Q. Noakes, P. Bailey, W. Allison, and P. C. Dastoor, Vacuum **73**, 115 (2004).
[15] D. A. MacLaren, P. C. Dastoor, R. T. Bacon, D. J. O'Connor, T. C. Q. Noakes, P. Bailey, and W. Allison, unpublished.
[16] S. Gallego, C. Ocal, and F. Soria, Surf. Sci. **377–379**, 18 (1997).
[17] M. Galeotti, A. Atrei, U. Bardi, B. Cortigiani, G. Rovida, and M. Torrini, Surf. Sci. **297**, 202 (1993).
[18] M. Sambi, E. Pin, and G. Granozzi, Surf. Sci. **340**, 215 (1995).
[19] J. W. M. Frenken, R. M. Tromp, and J. F. van der Veen, Nucl. Instrum. Methods Phys. Res. B **17**, 334 (1986).
[20] P. Gambardella and K. Kern, Surf. Sci. **475**, L229 (2001).
[21] A. F. Becker, G. Rosenfeld, B. Poelsema, and G. Comsa, Phys. Rev. Lett. **70**, 477 (1993).
[22] H. Röder, R. Schuster, H. Brune, and K. Kern, Phys. Rev. Lett. **71**, 2086 (1993).
[23] H. Röder, E. Hahn, H. Brune, J.-P. Bucher, and K. Kern, Nature (London) **366**, 141 (1993).
[24] P. Grütter and U. T. Dürig, Phys. Rev. B **49**, 2021 (1994).
[25] M.-F. Luo, D. A. MacLaren, I. G. Shuttleworth, and W. Allison, Chem. Phys. Lett. **381**, 654 (2003).